Acc. Chem. Res. **2005,** *38,* 283−291

Microporous Porphyrin Solids

KENNETH S. SUSLICK,* P. BHYRAPPA, J.-H. CHOU, MARGARET E. KOSAL, SHIRLEY NAKAGAKI, DENNIS W. SMITHENRY, AND SCOTT R. WILSON

School of Chemical Sciences, University of Illinois at Urbana-Champaign, 600 South Mathews Avenue, Urbana, Illinois 61801

Received July 7, 2004

ABSTRACT

Metalloporphyrins are exceedingly useful building blocks for the design and synthesis of molecularly based solids. The use of hydrogen bonding or metal ion coordination provides a wide range of framework solids. Using various polyfunctionalized porphyrins, we have created porous solids that are thermally robust and that retain their internal porosity upon loss of solvates. Their pore dimensions are comparable to zeolites, and they show shape and size selectivity in sorption of guest molecules and in epoxidation of alkenes.

Introduction

The thermal and chemical stability of metalloporphyrins make them attractive building blocks for the molecular engineering of solids with designed chemical, physical, or catalytic properties.[1] Our interest in this area goes back some 30 years to our studies of reversible O_2 binding in porous molecular solids of picket-fence metalloporphyrins[2−4] and especially our adventitious discovery of cooperativity in such binding for several such solids.[5,6] Planning and prediction of the structures of molecular solids, however, is notoriously difficult.

Recently, the rational design of porous solids[1,7−12] has been greatly advanced by the use of molecular "building blocks" linked in various coordination or organometallic frameworks. This approach has its roots in earlier work on one-dimensional coordination polymers.[13,14] Having channels and pores analogous to those found in zeolites, microporous (i.e., pores with diameters less than 20 Å) framework solids have the potential to perform shape-selective separations, chemical sensing, and catalysis.

Since the early 1990s, the synthesis of porphyrin framework solids has had major contributions from Robson,[15,16] Strouse,[17−21] Goldberg,[22−24] and Suslick and their co-workers.[1,25−32] Although there are many single crystal structures of porphyrinic solids that contain pores filled with generally disordered solvates, very few of these are stable to the removal of solvates. Nonetheless, the well-known homogeneous catalysis capabilities of metalloporphyrins,[33,34] especially for oxidation reactions, make porphyrin solids enticing targets for applications as heterogeneous catalysts. Selective sorption of small molecules and size- or shape-selective heterogeneous catalysis are clear goals for research on porphyrin framework solids, but only recently have successes come within range, and to date, *no example of a catalytic porphyrin framework solid has been reported*.

Porphyrins are easy to synthesize with multiple functionalities. This provides a diversity of open framework porphyrin structures that might be obtained through interporphyrin van der Waals interactions, hydrogen bonding, or metal−organic coordination bonding. In this Account, we will examine examples of all three approaches, with special emphasis of the success of the last approach.

Molecular Solids

The earliest recognition of porosity in metalloporphyrins was the discovery that the picket-fence porphyrins from Collman's group at Stanford reversibly bound O_2 in the solid state.[2−6] In the presence of solvate, these solids showed standard Langmuir isotherms with the formation of 1:1 complexes of O_2 to five-coordinate iron(II) or cobalt(II) porphyrin complexes of various imidazoles. The equilibrium binding constants of these porous solids were very similar to those of myoglobin and hemoglobin, depending on the steric demands of the coordinated imidazole.[2−4]

Remarkably, upon removal of the solvate by vacuum, the solids retained their porosity. Even more surprisingly, the O_2 binding of these solids became cooperative: the binding constant increased upon partial oxygenation of the solid, as shown in Figure 1.[5] The extent of the cooperativity and the binding constants (i.e., $P_{1/2}$) themselves were actually quite similar to mammalian hemoglobin.

The crystallographic structures of the (noncooperative) solvated solids were obtained[6] and provided some suggestions as to the source of the cooperative interactions.

Kenneth S. Suslick received his B.S. from Caltech and his Ph.D. from Stanford University. He is the *Marvin Schmidt* Professor of Chemistry and professor of Materials Science and Engineering at the University of Illinois at Urbana-Champaign. www.scs.uiuc.edu/suslick.

Puttaiah Bhyrappa received his Ph.D. at IISc−Bangalore, was a postdoctoral research associate at University of Southern California and then UIUC, and is currently assistant professor of chemistry at Indian Institute of Technology-Madras.

J.-H. Chou received his Ph.D. at Michigan State University and was a postdoctoral research associate at UIUC and is currently on staff at Merck Pharmaceuticals.

Margaret Kosal received her Ph.D. at UIUC and is currently a Scientific Fellow at Stanford in the Center for International Security and Cooperation.

Shirley Nakagaki received her Ph.D. from the University of São Paulo and is currently Professor of Chemistry at the Universidade Federal do Parana−UFPR, Brazil.

Dennis Smithenry received his Ph.D. from UIUC and is currently a postdoctoral research fellow at Stanford University.

Scott R. Wilson received his Ph.D. from UNC and is director of the G. L. Clark X-ray and 3M Materials Chemistry Facility of the UIUC.

* Corresponding author. E-mail: ksuslick@uiuc.edu.

10.1021/ar040173j CCC: $30.25
Published on Web 04/02/2005

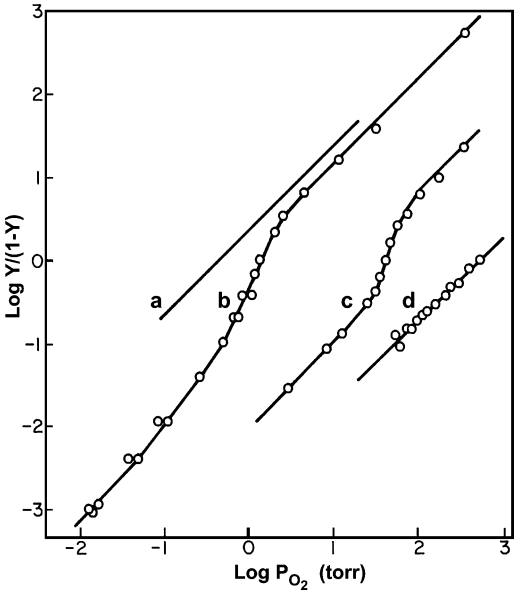

FIGURE 1. Hill plot of the uptake of O_2 by porous solids of picket-fence porphyrins:[5] (a) solid Fe(TpivPP)(1-MeIm); (b) Fe(TpivPP)(2-MeIm); (c) Fe(TpivPP)(1,2-Me_2Im); (d) Fe(T-pivPP)(2-MeIm)·C_2H_5OH. Plots b and c show cooperative O_2 binding in the solid-state comparable in magnitude to that of hemoglobin. TpivPP = 5,10,15,20-tetra(α,α,α,α-*o*-pivalamidophenyl)porphyrinate(−2), aka, picket-fence porphyrin. Im = imidazole.

Upon oxygenation, the axial imidazole is drawn roughly 0.5 Å toward the porphyrin plane, which in turn shortens the axes of the unit cell (Figure 2). Presumably in the nonsolvated solids, sufficient interaction exists between the metalloporphyrins to effect a cooperative phase transition in the solid state upon oxygenation. As molecules in the solid oxygenate, the change in molecular dimensions induces strain in the crystallite. Eventually this strain must be sufficient to induce a conformational change in the solid that enhances the dioxygen affinity of the remaining deoxy sites.[6]

To have true porosity, a solid must survive the removal of its solvates (or guests or inclusions or coordinating ligands). This is simply not the case for most molecular solids of porphyrins (including the misleadingly named "porphyrin sponges"[17−19]). Solids of the picket-fence porphyrins, however, remain one of the few exceptions. The interaction of small ligand binding with the solid-state structure is complex but gives rise to the still fascinating observation of cooperative ligation.

Hydrogen-Bonded Network Solids

The primary disadvantage of simple molecular solids, even of porphyrins, is that control of crystal structure is haphazard at best. The van der Waals interactions that hold picket-fence porphyrins or other "porphyrin sponge" solids[17−19] together are weak. The stability of such structures, particularly after removal of solvates, is highly problematic.

In an effort to synthesize more robust frameworks, we explored multiple hydrogen-bond interactions as the basis for linking porphyrin molecules. Hydrogen bonds offer the additional advantages of directionality and selectivity. In particular, we examined a series of solids based on symmetrically substituted octahydroxyporphyrins.[25,26] The octahydroxyporphyrins were chosen for two reasons. First, we expected to gain more rational control the structure of porphyrinic solids through the three-dimensional disposition of hydroxyl groups on both faces of the porphyrin (relative, say to the flat tetra(4-hydroxy phenyl)porphyrin[20]). Second, we hoped to enhance the solids' stability by creating eight hydrogen bonds per porphyrin.

These supramolecular network solids were stabilized by hydrogen bonding between either *ortho*- or *meta*-dihydroxyphenylporphyrins (Figure 3) and their Zn(II) and Mn(III) derivatives. The position of the peripheral hydroxyl groups, the choice of metalated or free base porphyrin, and the nature of the solvate dramatically influence structural features and give rise to a diversity of fascinating structures. These materials also feature significant void volumes (but only *theoretical* voids, as it turns out), as high as 67% calculated solvate and channel volume from the X-ray crystal structures.

The obvious structure for such hydrogen-bonding molecules is a simple columnar stack, and in fact, a one-dimensional hydrogen-bonding structure was found for H_2(T(3′,5′-DHP)P)·5EtOAc. These columns of porphyrins align parallel to one another, forming a porous three-dimensional network with channels of 6.5 Å × 6.5 Å (van der Waals surface to van der Waals surface) between them and 3.4 Å × 3.4 Å running perpendicular to the columns (Figures 4 and 5).

The interactions between the columns are weak van der Waals interactions. Consequently, the columnar stacks do not tolerate large solvates; however, when benzonitrile is used as the solvent for crystallization, the structure of H_2(T(3′,5′-DHP)P)·$7C_6H_5CN$ changes substantially to a two-dimensional array of porphyrins interconnecting via hydrogen bonds generating a three-dimensional corrugated-sheet configuration. The observed variation in solid-state structure reflects the steric requirements necessitated by the larger benzonitrile guest molecules.

When the hydroxyl substituents are simply changed from the *meta*- to the *ortho*-phenyl positions, an essentially two-dimensional layered material results. The peripheral hydroxyl groups of H_2(T(2′,6′-DHP)P)·4EtOAc induce a slight ruffling of the porphyrin macrocyclic rings and show strong directional hydrogen bonding (Figure 6). Channels 3.0 Å × 3.6 Å wide were formed by the packing of the layers.

Both the Zn(II) and Mn(III) derivatives of these porphyrins produce interesting framework solids. Zn(T(3′,5′-DHP)P)$(THF)_2$·2THF·$3CH_2Cl_2$ has a layered motif in which the metalloporphyrins are arranged in a "slipped stack" orientation of flat porphyrin planes held together by hydrogen bonding (Figure 7). The interplanar separation between the hydrogen-bonded neighbors in a given layer is 6.81 Å, and the nearest neighbor in the adjacent layer is offset by a vertical distance of 4.98 Å from the

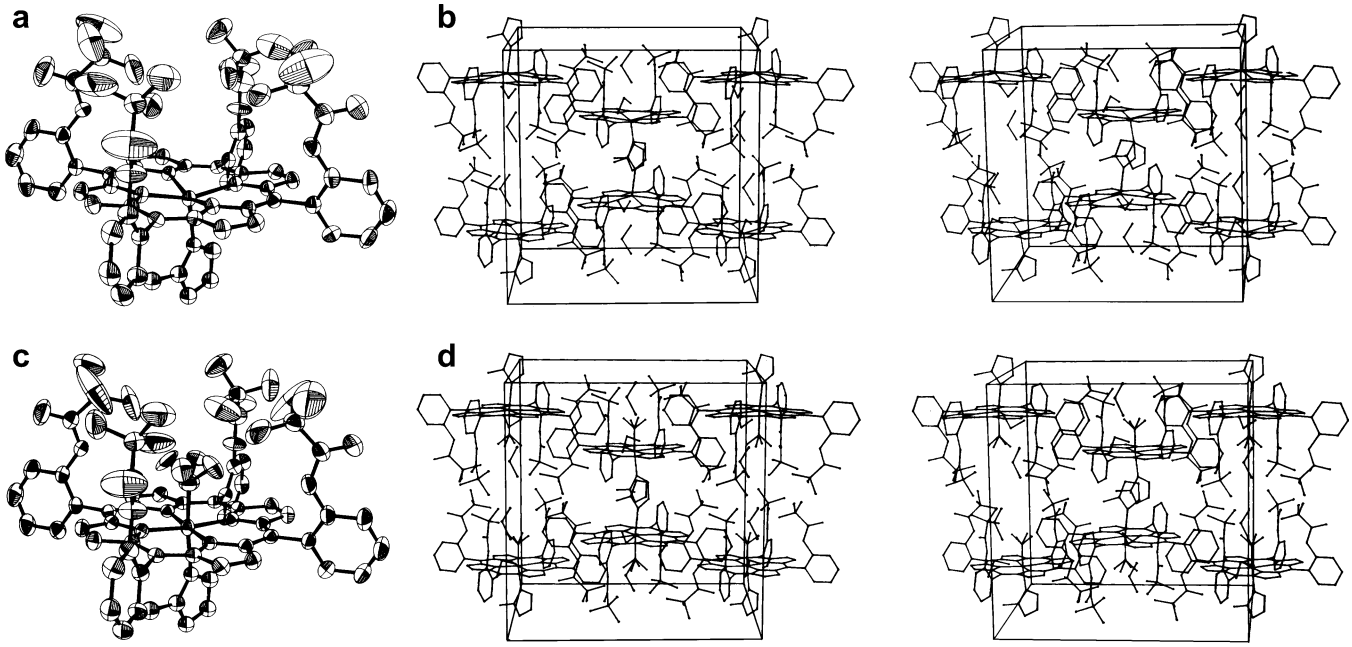

FIGURE 2. Single-crystal X-ray structures[6] of Fe(TpivPP)(2-MeIm)·C_2H_5OH, (a) ORTEP of single molecule and (b) stereoview of crystal packing structure, and Fe(TpivPP)(2-MeIm)(O_2)·C_2H_5OH, (c) ORTEP of single molecule and (d) stereoview of crystal packing structure.

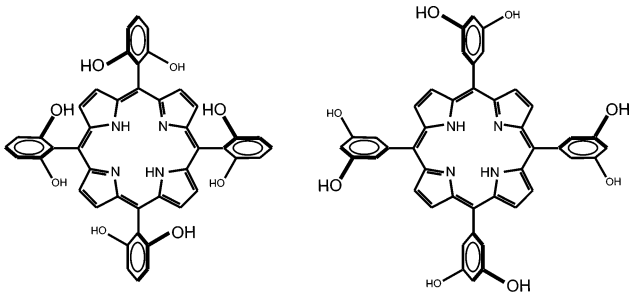

FIGURE 3. Hydrogen-bonding porphyrin building blocks for network solids: left, H_2(T(2′,6′-DHP)P) (5,10,15,20-tetrakis(2′,6′-dihydroxyphenyl)porphyrin); right, H_2(T(3′,5′-DHP)P) (5,10,15,20-tetrakis-(3′,5′-dihydroxyphenyl)porphyrin).

porphyrin plane. The *ortho*-substituted complex, Zn-[T(2′,6′-DHP)P] $(EtOAc)_2$·2 EtOAc, has a very similar structure.

In the structure of Mn(T(3′,5′-DHP)P)(Cl)·2EtOAc, a new type of layered structure is found, in which it is the chloride anions that hold the planes together. Each chloride anion bridges four hydroxyl groups from four separate porphyrins in a square planar arrangement with an average Cl···O distance of 3.01 Å creating a two-dimensional array (Figure 8). Hydrogen bonding between layers generates a three-dimensional network with 4.6 Å × 3.4 Å wide channels.

While hydrogen bonding is certainly a stronger interaction than the van der Waals interactions that hold molecular solids together, it still provides only modest stabilization of the solids in the absence of their solvates. Even with our octahydroxy porphyrins, the stabilities of the solids are limited. The crystal structures that we find for the hydrogen-bonded networks are certainly beautiful, and they are open frameworks without the interpenetration so common in pseudo-porous frameworks. Yet even with eight hydrogen bonds per porphyrin, the hydrogen-bonded structures are not robust. Upon removal of solvates by vacuum, the solids no longer diffract X-rays, and the structure collapses leaving no real porosity.

Robust Microporous Solids

To make robust porous solids (i.e., frameworks that remain intact after removal of solvates), one must make linkages between the molecular building blocks that are truly substantial (e.g., greater than the ~32 kcal that eight hydrogen bonds might be worth). While covalent organic bonds might be contemplated, the inherent difficulty in permitting equilibration of such bonds between units during crystallization leads to amorphous and ill-defined polymers. The weaker bonds of coordination metal complexes and organometallic compounds fill the ideal middle ground for the synthesis of robust solids.

Crystallography by itself, of course, is not sufficient to evaluate the porosity of such solids. Functional porosity must be evaluated by techniques that actually measure sorption: for example, thermal gravimetric analysis (TGA) or gas adsorption studies (sometimes referred to as BET). Furthermore, such studies must be done over a series of sorption−desorption to show that the framework retains microporosity upon evacuation. In an ideal case, crystallinity may also be retained at the micrometer scale, in which case powder or single crystal X-ray diffraction (XRD) can establish quantitatively the nature of the structural changes. Robust microporosity, however, does not require long range order sufficient for good XRD.

We approached the synthesis of robust porphyrin solids with the rationale that if we wanted zeolite-like materials, then we should try to make them in a zeolite-like manner. To this end, we explored moderately high-temperature solvothermal routes involving polyfunctionalized porphyrin building blocks.

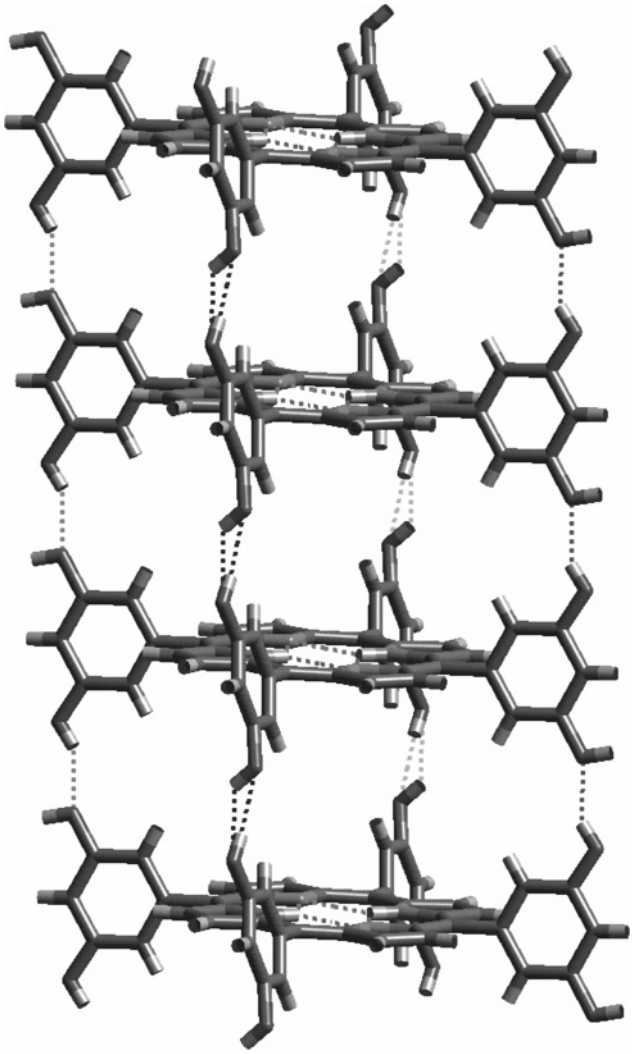

FIGURE 4. Molecular packing diagram of H_2T(3′,5′-DHP)P·6EtOAc showing one-dimensional columnar structure.[25] Hydrogen bonding interactions between the hydroxyl groups are shown with dotted lines.

Our first success came with the synthesis of a non-interpenetrating framework solid, dubbed PIZA-1 (porphyrinic Illinois zeolite analogue-1), made up of ruffled cobalt(III) tetra(*p*-carboxyphenyl)porphyrins (TpCPP) coordinated in three dimensions to linear trinuclear cobalt(II) clusters.[29] PIZA-1 was prepared solvothermally by heating a mixture of free-base porphyrin acid and cobaltous chloride in a sealed tube with pyridine/KOH (0.1 M, aq) at 150 °C for 2 days. Oxidation states in these systems were confirmed both by charge balance and by close examination of the metal−ligand bond lengths.

The crystal structure indicates that there are 7 Å × 14 Å channels down the crystallographic *a* axis and 7 Å × 9 Å channels down both the *b* and *c* axes, creating a open framework with an impressive void volume of 74%. The molecular diagrams in Figure 9 illustrate these channels, which contain disordered pyridine and water molecules in the as-synthesized state.

The PIZA-1 porosity is thermally robust as evidenced by XRD, TGA, and nitrogen adsorption studies. Thermal gravimetric analysis indicated a significant (60%) weight loss upon first time heating attributable to loosely held solvate molecules and coordinated pyridine and water molecules; as discussed below, multiple cycles (>10) of sorption/thermal desorption of various solvates indicates excellent reversibility. Further proof of the stability of the evacuated material was obtained via a series of nitrogen

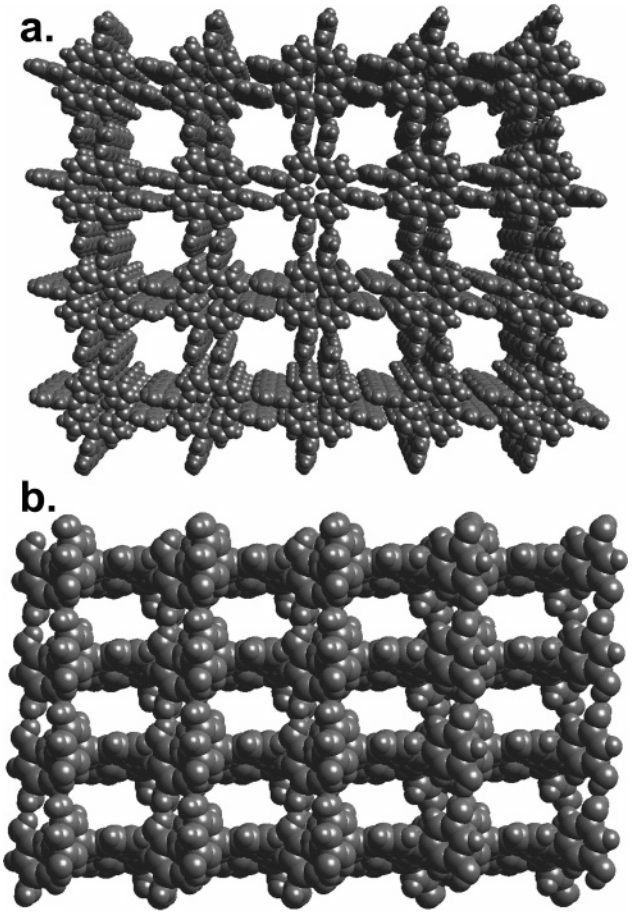

FIGURE 5. Molecular packing diagrams of H_2T(3′,5′-DHP)P·5EtOAc (van der Waals spheres shown at 0.7 of atomic radii):[25] (a) showing channels of 6.5 Å by 6.5 Å, between the columns; (b) showing channels of 3.4 Å by 3.4 Å running perpendicular to the columns. Solvent molecules are not shown for clarity.

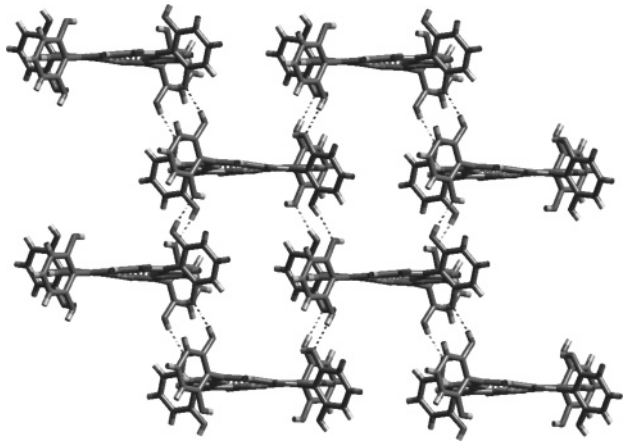

FIGURE 6. Molecular packing diagram of H_2T(2′,6′-DHP)P·4EtOAc showing a two-dimensional layered structure.[25,26] Hydrogen bonding interactions between the hydroxyl groups are shown with dotted lines. Solvent molecules are not shown for clarity.

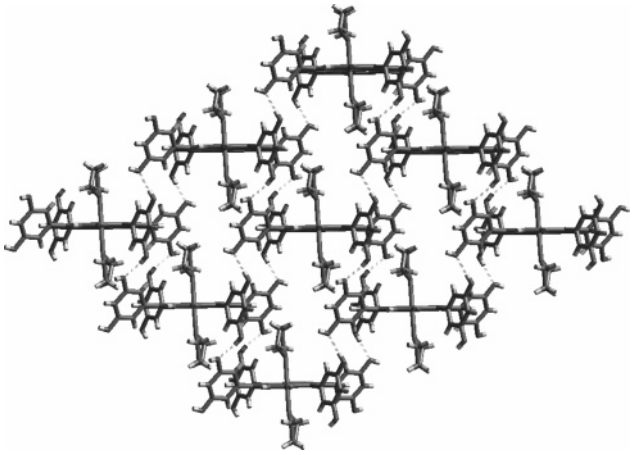

FIGURE 7. Two-dimensional layer from the crystal structure[25,26] of $Zn[T(3',5'\text{-}DHP)P](THF)_2 \cdot 2THF \cdot 3CH_2Cl_2$. Noncoordinated solvates are not shown for clarity.

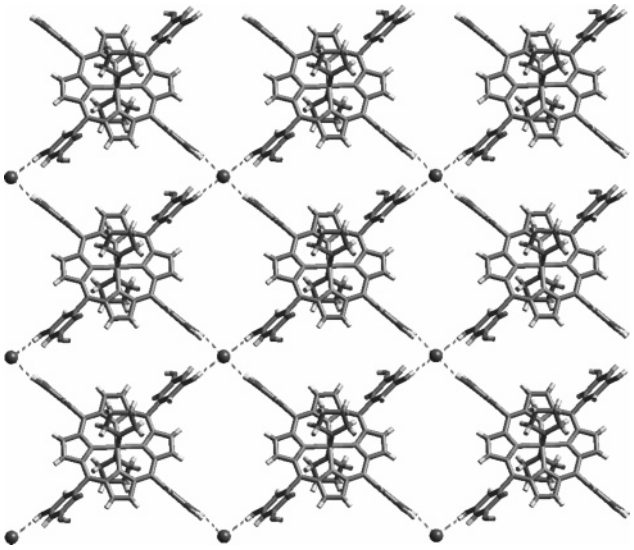

FIGURE 8. Molecular packing diagrams[25] of $Mn[T(3',5'\text{-}DHP)P](THF)_2 \cdot Cl \cdot 2THF \cdot 5C_6H_5CH_3$ showing two-dimensional sheets of porphyrins (001 plane) linked by unusual square-planar Cl^- anions hydrogen bonding to four metalloporphyrins. Spheres indicate bridging chloride ions. Solvate molecules and coordinated THF ligands are not shown for clarity.

adsorption studies on microcrystalline material. PIZA-1 is thermally stable in a vacuum to >250 °C for days, and decomposition begins during TGA at ~375 °C.

Molecular modeling of the evacuated network of PIZA-1 revealed an exceptionally large van der Waals void volume of 73.9% (7559 Å^3 per unit cell). The calculated accessible free volume is 47.9% (4905 Å^3 per unit cell) for a 1.40 Å probe radius (i.e., water). Comparative calculations done using the same methods for zeolite 4A resulted in much smaller accessible volumes for all physically meaningful probe radii (e.g., 27.2% for a 1.40 Å probe radius).

Consistent with the molecular modeling, PIZA-1 possesses extraordinary properties as a desiccant for selective drying of common organic solvents (e.g., benzene, toluene, and tetrahydrofuran), as shown in Figure 10. In a comparison to 4 Å molecular sieves (zeolite 4A), PIZA-1 demonstrated *both* greater capacity and higher affinity

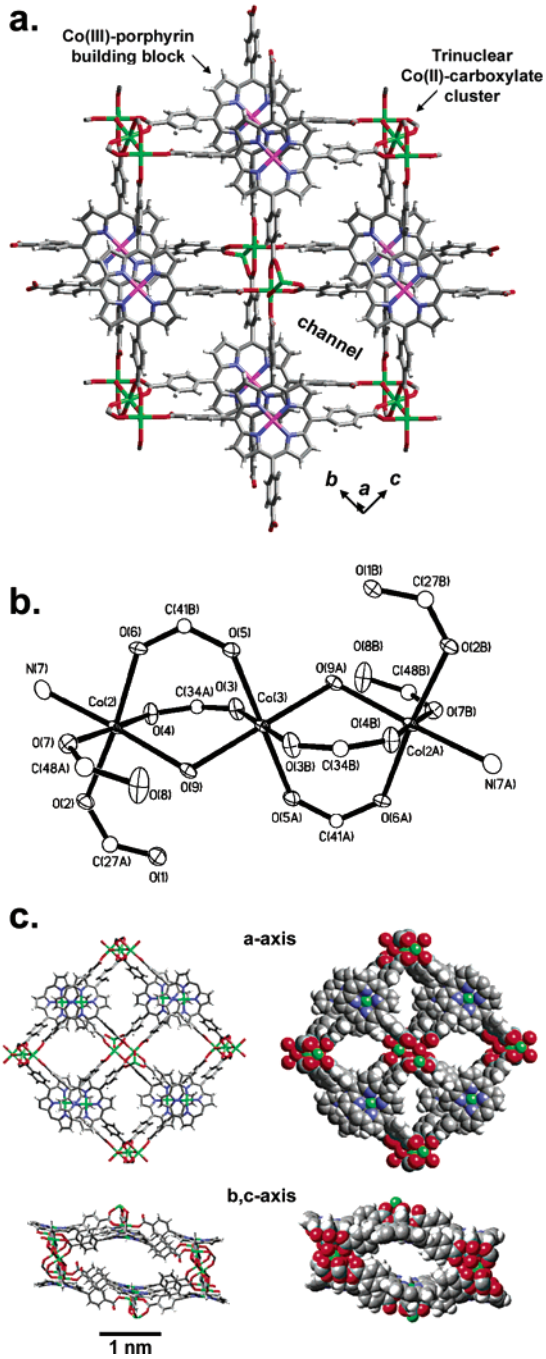

FIGURE 9. Molecular diagram (a) of PIZA-1 network viewed along *a*-axis showing connectivity leading to formation of 30.8 Å × 30.8 Å × 10.0 Å internal voids (van der Waals surface to van der Waals surface) at the intersection of tri-directional channels.[29] X-ray structure from single crystals of $[Co(TpCPP)Co_{1.5}(C_5H_5N)_3(H_2O)] \cdot 11C_5H_5N$ at 198 K. In panel b, linear trinuclear Co(II)-carboxylate clusters, $[Co^{II}_3(C_5H_5N)_2(H_2O)_2(O_2C{-}Porph)_8]$, link the eight metalloporphyrin building blocks. Co(2)−Co(3)−Co(2A) angle = 180.0(3)°. In panel c, a space-filling model reveals four channels (13.8 Å × 6.8 Å) per unit cell along the crystallographic *a*-axis and oval-shaped channels (9.3 Å × 7.4 Å) along the *b*- and *c*-axes. Ruffled porphyrin macrocycles are perpendicular to the plane of the paper. Spheres represent 70% van der Waals radii.

with faster response for the selective sorption of water. PIZA-1 acted as a better desiccant in 1 h than 4 Å molecular sieves did in 1 day.

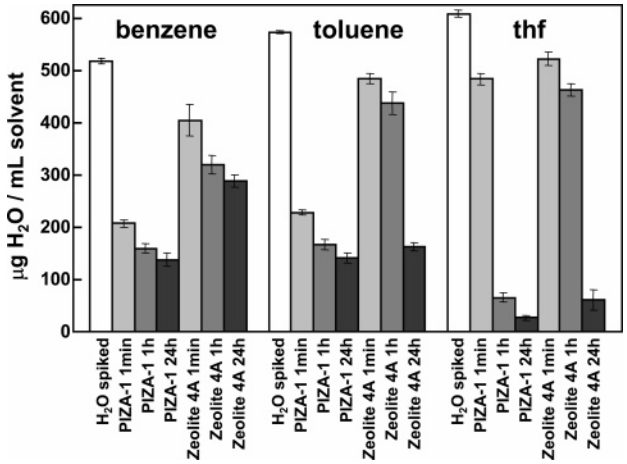

FIGURE 10. Selective adsorption of water from benzene, toluene, and tetrahydrofuran (THF) solutions, determined via Karl–Fischer coulometric titration.[29] Organic solvents were saturated with water under N_2. Fifty milligrams of PIZA-1 or 4 Å molecular sieves (zeolite 4A), pretreated and ground, were stirred in a flask under N_2. Based on thermal desorption studies, 1.05 g of H_2O is absorbed per gram of PIZA-1 at equilibrium, but only 0.22 g of H_2O per gram of zeolite 4 Å is absorbed.

PIZA-1 shows some remarkable selectivities in its sorption abilities. There is a clear analogy to be drawn here between the use of hindered metalloporphyrins in solution (e.g., bis-pocket porphyrins and dendrimer porphyrins[35–39]) and the use of the solid state packing to provide similar steric control. Selectivity with regard to hydrophilicity of guest species, guest size, and guest shape was probed by monitoring gravimetrically the thermal desorption of a variety of guests (Figure 11a) from the fully desolvated network. PIZA-1 shows a very strong selectivity for hydrophilic guests and absorbs water, amines, and alcohols preferentially. Hexane and less polar functionalized hexanes are not adsorbed significantly. The low absorption of hexanoic acid initially appears anomalous but likely reflects the strong tendency of carboxylic acids to form large hydrogen-bonded dimers.

Sorption of amines provided a platform to explore the shape and size selectivity of PIZA-1 (Figure 11a,b). For the series of linear alkylamines ($C_nH_{2n+1}NH_2$), chain length makes a substantial impact on the extent of sorption. Short-chain alkylamines ($n = 4$, 5, or 6) were adsorbed to the greatest extent. As chain length increases ($n = 7$, 8, 10) a progressive decrease in sorption was observed. Size selectivity was examined via sorption studies on a series of progressively larger aromatic amines: pyridine > aniline > 3,5-dimethylaniline > 4-*tert*-butylpyridine > 2,4,6-collidine.

Shape selectivity was probed using the picoline series (methyl pyridines, $C_5H_4(CH_3)N$). Steric hindrance paralleled the observed sorption: the least sterically hindered, 4-picoline, was absorbed more than 3-picoline, which was absorbed more than the most sterically hindered, 2-picoline. Shape selectivity was also examined by observing the sorption of the isomers of butyl-substituted amines: the least hindered *n*-butylamine was absorbed much more than di-*n*-butylamine, which was absorbed much more than the increasingly sterically hindered di-*iso*-, di-*sec*- and di-*tert*-butylamines (Figure 11b). As the bulky organic substituents encroach upon the hydrophilic group, guest sorption declines.

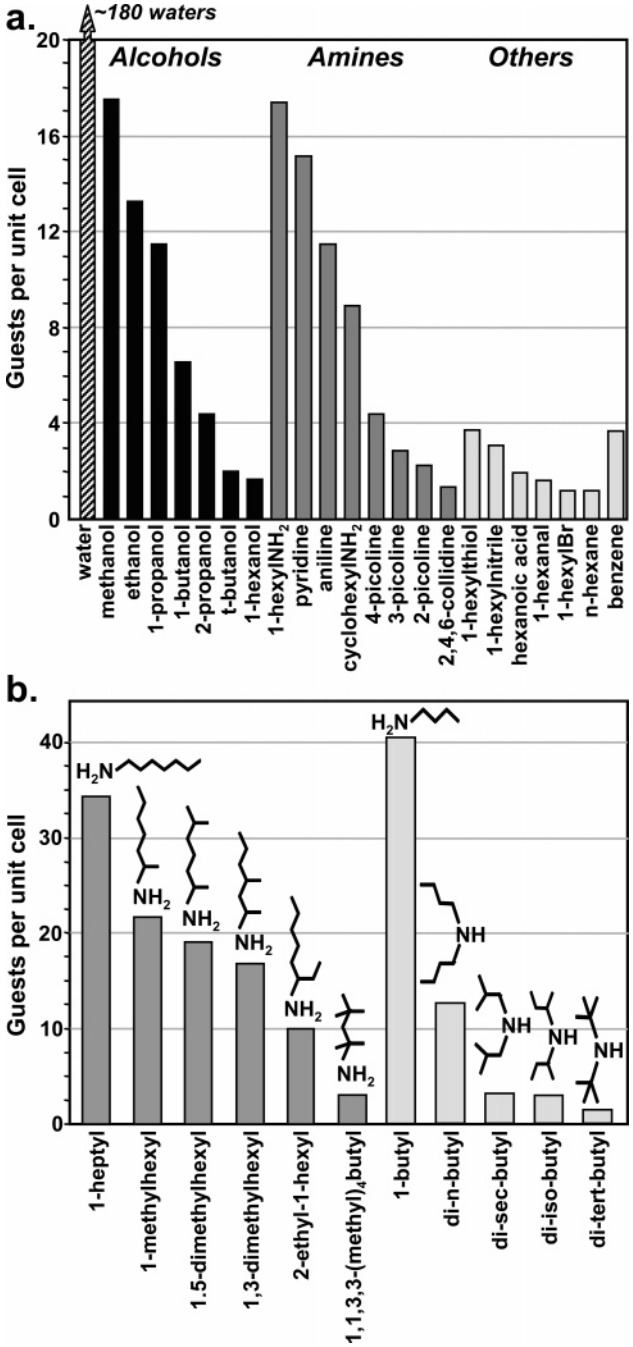

FIGURE 11. Size, shape, and functional-group selectivity (a) as probed by thermal desorption of guest molecules using TGA.[29] Prior to guest exposure, solids were degassed 24 h at 275 °C in vacuo. Panel b shows size and shape selectivity within the butylamine series at near-saturation exposure levels (right side). As the hydrophilic amine group is more sterically congested, sorption is observed to decline. Comparison of sorption of unsubstituted (1-heptyl) and substituted alkylamine isomers further demonstrates the shape-selective sorption behavior of PIZA-1 (left side).

Two other closely related porphyrin frameworks have also been characterized.[31] PIZA-2 contains cobalt(III) tetra(*p*-carboxyphenyl)porphyrins that coordinate to a bent

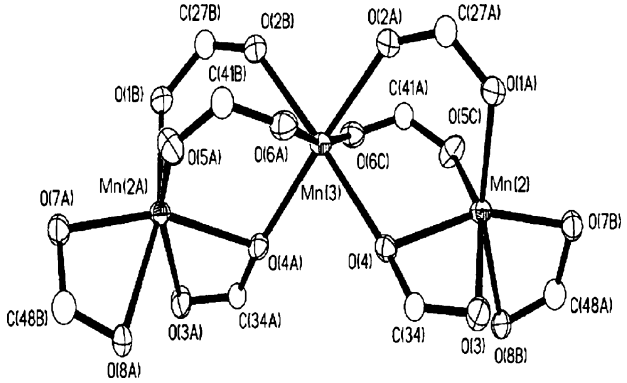

FIGURE 12. ORTEP diagram showing the bent trinuclear Mn(II)-carboxylate coordination of PIZA-3.[31] Each trinuclear cluster is coordinated by eight separate Mn(III)-porphyrin carboxylate moieties; each Mn(III)-porphyrin carboxylate coordinates four distinct Mn(II) trinuclear clusters.

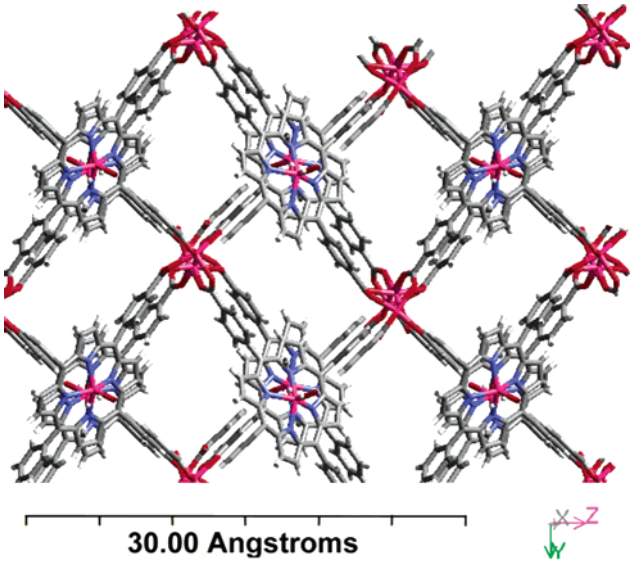

FIGURE 13. The PIZA-3 network, $(Mn(TpCPP)Mn_{1.5})(C_3H_7NO)\cdot 5C_3H_7NO$, viewed along the crystallographic *a*-axis.[31] Solvate and coordinated *N,N*′-dimethylformamide molecules have been removed for clarity.

trinuclear cobalt cluster. PIZA-3 is isostructural to PIZA-2 but instead contains manganese(III) tetra(*p*-carboxyphenyl)porphyrins and a bridging bent trinuclear manganese cluster (Figure 12). A molecular diagram of the PIZA-3 framework is shown in Figure 13. There are alternating 5 Å × 9 Å and 7 Å × 8 Å pores down the crystallographic *a* axis and 3 Å × 5 Å pores down the *c* axis, creating an open framework with 56% void volume. PIZA-3 shows sorption characteristics similar to PIZA-1: a strong preference for small, slender, hydrophilic guests.

Of some interest, PIZA-3 is a capable and robust oxidation catalyst for the hydroxylation of a variety of linear and cyclic alkanes and the epoxidation of cyclic alkenes (Table 1). Yields were similar to other manganese porphyrins in homogeneous systems or immobilized inside inorganic supports as heterogeneous catalysts.[33,34] Similar results were also observed using peracetic acid as the oxidizing source. The catalyst is oxidatively robust. After the oxidation reaction, the supernatant was analyzed

Table 1. Distribution of the Main Reaction Products in the Oxidation Reactions Catalyzed by PIZA-3 Using Iodosylbenzene as Oxidant

substrate	% yield of products[a]		
cyclic alkanes	alcohol	ketone	alcohol/ketone
cyclohexane	43	4.8	8.9
cycloheptane	47	5.9	8.0

substrate	% yield of products[a]	
cyclic alkenes	epoxide	allylic products
cyclooctene	74	*e*
cyclohexene	23	*e*
cyclopentene	23	*e*
limonene	20[b]	*e*

substrate	% yield of products[a]			
linear alkanes and others	2-ol	3-ol	4-ol	aldehyde
hexane	7.0	10	*e*	*e*
heptane	8.0	10	5.0	
3-methyl-butane	27[c]			*e*
1-hexanol				17[d]

[a] Yield based on iodosylbenzene. Reaction conditions: catalyst: oxidant:substrate:imidazole molar ratio = 1:10:1000:1, solvent acetonitrile, magnetic stirring for 2h at room temperature. [b] Limonene epoxide cis and trans mixture obtained from the oxidation of the ring position 1,2. [c] 3-methyl-2-butanol. [d] 1-Hexanal was the major product; <5% 1,2-hexane-diol was observed. [e] Not detected.

by UV−vis spectroscopy, and no traces of metalloporphyrin or degradation products were observed (<0.1 μM). In addition, after use as oxidation catalyst and isolation by filtration, the used catalyst showed no significant loss of activity with peracetic acid as oxidant source.

The size- and shape-selective oxidation reactivity of PIZA-3 was evaluated, but unfortunately, no shape selectivity is observed in these initial catalytic studies. Because shape-selective sorption has been demonstrated both with PIZA-3 (discussed earlier) and with the related PIZA-1, we suspect that the lack of shape selectivity (Table 1) is due to catalysis occurring on the exterior surface of the crystalline material rather than inside the pores. Indeed, the addition of bases capable of coordinating to surface Mn porphyrin sites but too peripherally bulky to fit into the pores (e.g., 3,5-di-bromo-pyridine or 1-phenyl-imidazole) substantially slows the catalytic oxidation. Thus, the lack of shape-selective oxidation may simply reflect that the pores of PIZA-3 are hydrophilic and unable to sorb nonpolar substrates into the internal pores of the framework. Further work on the synthesis of porphyrin framework solids with more hydrophobic channels is ongoing.

The need for more hydrophobic microporosity has led us to a robust microporous zinc porphyrin framework solid.[32] Building upon Yaghi and co-workers' recent report[40] of porous Zn_4O-bridged arene-dicarboxylate framework solids, a Zn_4O framework with zinc(II) *trans*-bis(carboxylate)porphyrin bridges has been synthesized. The structural model of the solid, which we designate PIZA-4, contains an interpenetrated cubic framework of zinc(II) *trans*-carboxylateporphyrins that coordinate the edges of tetrahedral Zn_4O clusters as shown in Figure 14.

Even with this interpenetration, the framework solid is largely open with 74% free volume (calculated for a

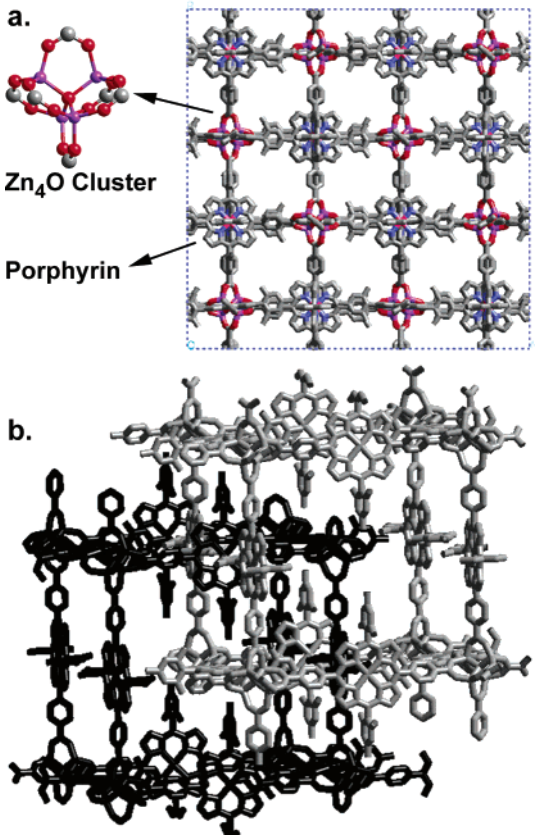

FIGURE 14. Crystal structure of interpenetrated PIZA-4 (a) average view down cubic axis.[32] Hydrogens are omitted for clarity. Enlargement shows coordination of six carboxylates from the metalloporphyrins to the Zn_4O tetrahedral cluster. The metalloporphyrin groups are 5,15-di(*p*-carboxyphenyl)-10,20-di(2′,4′,6′-trimethylphenyl)porphyrinatozinc(II). Panel b shows the two interpenetrating frameworks of PIZA-4. One framework is shaded darker.

1.4 Å probe radius) and 4 Å × 7 Å pores down each axis. In the solvated crystal, the pores are filled with disordered solvate. This large free volume was confirmed by TGA measurements on the as-synthesized solvated crystal. A measured weight loss of 32% (up to 250 °C) is equivalent to 134 DMF and 102 chlorobenzene molecules occupying each unit cell, which corresponds to 100% of the calculated accessible free volume being occupied.

PIZA-4 is microporous and thermally robust. Solvates were completely removed by heating at 250 °C under vacuum, and minimal further weight loss occurs up to 400 °C. To determine the nature of evacuated PIZA-4, reversible type I N_2 isotherms at 77 K were measured for the desolvated PIZA-4 solids and are consistent with microporosity. A Langmuir surface area of 800 m^2/g, calculated from the isotherm data, compares favorably to the ~500 m^2/g for a typical zeolite. The evacuated solid also reversibly resorbs 241 *N*,*N*-dimethylformamide molecules per unit cell, which corresponds to 94% of the accessible free volume calculated from the single-crystal model. These two findings indicate that the pores remain open and available for resorption of solvate.

Furthermore, the XRD peaks for evacuated PIZA-4 powder are broadened and shifted when compared to the initial solvated sample but still show substantial long-

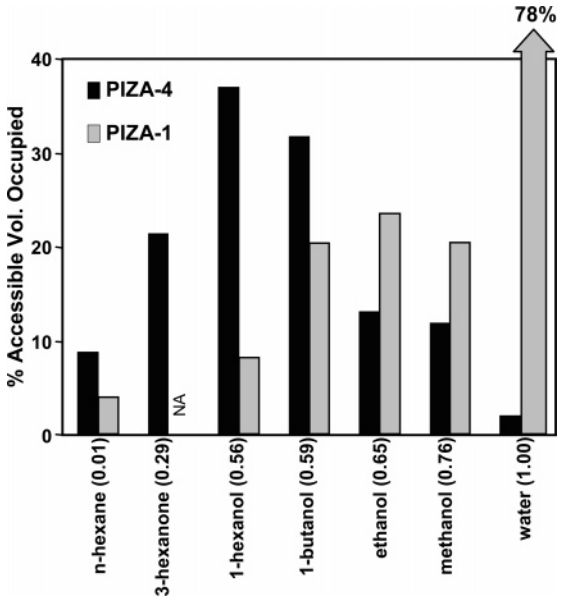

FIGURE 15. PIZA-4 and PIZA-1 sorption data for substrates of increasing polarity.[32] E_T^N solvent polarity values given in parentheses (3-hexanone value approximated from that of 2-hexanone).[41]

range order. Reexposure of the evacuated PIZA-4 powder to *N*,*N*-dimethylformamide/chlorobenzene resolvates the solid, and the original XRD powder pattern for PIZA-4 returns within a few minutes. Because the solid is completely insoluble (less than micromolar), the resolvation does not involve dissolution/recrystallization but rather a direct diffusion of solvates back into the pores of the framework solid.

Results from TGA analysis of solvate desorption (Figure 15) indicate that PIZA-4 is selective toward adsorption of substrates with medium polarity, which is in striking contrast to the very polar pores of PIZA-1. Further control is possible through alteration of the non-carboxylate phenyl groups of the porphyrins; the 10,20-mesityl groups in the current solid provide a means to control the shape and moderate polarity of the solids' pore structure. Very recent work with the Mn(III) porphyrin analogue of PIZA-4 suggests that this will be a promising shape-selective catalyst for organic oxidations.[32]

Conclusions

The development of robust microporous framework solids has the potential to perform selective small-molecule sorption or heterogeneous catalysis with size or shape selectivity. Despite the very large number of framework solid state structures, there remain only a very few examples where the solids are *robust* and retain porosity after loss of solvates.

Porphyrin solids have a long history of microporosity, with reversible O_2 binding in picket-fence metalloporphyrins remaining a prime example. The structures of molecular solids, however, are difficult to control or predict. Multiple hydrogen bonding between polyfunctionalized porphyrins provides an alternative for rational crystal design. Diverse solid state structures have been

created in this fashion, but even eight hydrogen bonds fail to generate truly robust porous solids.

The stronger intermolecular interactions afforded by metal ion coordination to carboxylates on the porphyrin periphery are sufficient, fortunately, to generate exceptionally robust solids. Metalloporphyrin framework solids held together by such coordination (which we call PIZAs) retain their porosity and sometimes even their long-range crystallinity after loss of all solvates and up to temperatures >300 °C. The sorption abilities of these solids are impressive. PIZA-1, for example, has *both* greater capacity and higher affinity with faster response for the selective sorption of water than standard molecular sieves; in fact, PIZA-1 is a better (albeit not cheaper!) desiccant for solvent drying in 1 h than 4 Å molecular sieves are in 1 day. In addition, we have been able to control the selectivity of sorption in terms of guest hydrophobicity, size, and shape by generating a range of different pore dimensions. Initial studies of hydrocarbon oxidations using these porphyrins show them to be robust heterogeneous catalysts. Modification of the porphyrin periphery should permit further tuning of the sorptive and catalytic properties of these robust microporous solids.

This work was supported by the U.S. NIH (Grant HL 25934) and by the DOE Seitz Materials Research Laboratory under Grant DEFG02-91-ER45439.

References

(1) Chou, J.-H.; Kosal, M. E.; Nalwa, H. S.; Rakow, N. A.; Suslick, K. S. Applications of porphyrins and metalloporphyrins to materials chemistry. In *The Porphyrin Handbook*; Kadish, K. M., Smith, K. M., Guilard, R., Eds.; Academic Press: New York, 2000; Vol. 6, Chapter 41, pp 43−131.

(2) Collman, J. P.; Halbert, T. R.; Suslick, K. S. O_2 binding by metalloporphyrins. In *Metal Ion Activation Of Dioxygen*; Spiro, T. G., ed.; Prentice Hall: New York, 1980; pp 1−72.

(3) Collman, J. P.; Brauman, J. I.; Suslick, K. S. Oxygen binding to iron porphyrins. *J. Am. Chem. Soc.* **1975**, *97*, 7185−7186.

(4) Collman, J. P.; Brauman, J. I.; Doxsee, K. M.; Halbert, T. R.; Hayes, S. E.; Suslick, K. S. Oxygen binding to cobalt porphyrins. *J. Am. Chem. Soc.* **1978**, *100*, 2761−2766.

(5) Collman, J. P.; Brauman, J. I.; Rose, E.; Suslick, K. S. Cooperativity in oxygen binding to iron porphyrins. *Proc. Natl. Acad. Sci. U.S.A.* **1978**, *75*, 1052−1055.

(6) Jameson, G. B.; Molinaro, F. S.; Ibers, J. A.; Collman, J. P.; Brauman, J. I.; Rose, E.; Suslick, K. S. Models for the active site of oxygen binding hemoproteins. Dioxygen binding properties and the structures of (2-Methylimidazole)-meso-tetra(α,α,α,α-o-pivalamidophenylporphyrinatoiron(II)−Ethanol and Its dioxygen adduct. *J. Am. Chem. Soc.* **1980**, *102*, 3224−3237.

(7) Pinnavaia, T. J.; Thorpe, M. F. In *Access in Nanoporous Materials*; Thorpe, M. F., Ed.; Plenum: New York, 1995.

(8) Aoyama, Y. Functional organic zeolite analogues. *Top. Curr. Chem.* **1998**, *198*, 131−161.

(9) Cheetham, A. K.; Ferey, G.; Loiseau, T. Open-framework inorganic materials. *Angew. Chem., Int. Ed.* **1999**, *38*, 3268−3292.

(10) Barton, T. J.; Bull, L. M.; Klemperer, W. G.; Loy, D. A.; McEnaney, B.; Misono, M.; Monson, P. A.; Pez, G.; Scherer, G. W.; Vartuli, J. C.; Yaghi, O. M. Tailored porous materials. *Chem. Mater.* **1999**, *11*, 2633−2656.

(11) Langley, P. J.; Hulliger, J. Nanoporous and mesoporous organic structures: new openings for materials research. *Chem. Soc. Rev.* **1999**, *28*, 279−291.

(12) Eddaoudi, M.; Moler, D. B.; Li, H.; Chen, B.; Reineke, T. M.; O'Keeffe, M.; Yaghi, O. M. Modular Chemistry: Secondary building units as a basis for the design of highly porous and robust metal-organic carboxylate frameworks. *Acc. Chem. Res.* **2001**, *34*, 319−330.

(13) Chen, C.-T.; Suslick, K. S. One-dimensional coordination polymers. *Coord. Chem. Rev.* **1993**, *128*, 293−322.

(14) Bailar, J. C., Jr. Coordination polymers. In *Preparative Inorganic Reactions*; Jolly, W. L., Ed.; Interscience: New York, 1964; Vol. 1, pp 1−25.

(15) Abrahams, B. F.; Hoskins, B. F.; Robson, R. A new type of infinite 3D polymeric network containing 4-connected, peripherally linked metalloporphyrin building blocks. *J. Am. Chem. Soc.* **1991**, *113*, 3606−3607.

(16) Abrahams, B. F.; Hoskins, B. F.; Michall, D. M.; Robson R. Assembly of porphyrin building blocks into network structures with large channels. *Nature (London)* **1994**, *369*, 727−729.

(17) Dastidar, P.; Stein, Z.; Goldberg, I.; Strouse C. E. Supramolecular assembly of functionalized metalloporphyrins−porous crystalline networks of zinc-tetra(4-carboxyphenyl)porphyrin. *Supramol. Chem.* **1996**, *7*, 257−270.

(18) Byrn, M. P.; Curtis, C. J.; Goldberg, I.; Hsiou, Y.; Khan, S. I.; Sawin, P. A.; Tendick, S. K.; Strouse, C. E. Porphyrin sponges: structural systematics of the host lattice. *J. Am. Chem. Soc.* **1991**, *113*, 6549−6557.

(19) Byrn, M. P.; Curtis, C. J.; Hsiou, Y.; Khan, S. I.; Sawin, P. A.; Tendick, S. K. Terzis, A.; Strouse, C. E. Porphyrin sponges: conservative of host structure in over 200 porphyrin-based lattice clathrates. *J. Am. Chem. Soc.* **1993**, *115*, 9480−9497.

(20) Byrn, M. P.; Curtis, C. J.; Hsiou, Y.; Khan, S. I.; Sawin, P. A.; Terzis, A.; Strouse, C. E. Porphyrin-based lattice clatrates. *Comprehensive Supramol. Chem.* **1996**, *6*, 715−732.

(21) Krupitsky, H.; Stein, Z.; Goldberg, I.; Strouse, C. E. Coordination polymers and aggregation modes of tetra(4-pyridylporphyrin. *J. Inclusion Phenom.* **1994**, *18*, 177−192.

(22) Goldberg, I. Metalloporphyrin molecular sieves. *Chem.−Eur. J.* **2000**, *6*, 3863−3870.

(23) Goldberg, I. Design Strategies for Supramolecular Porphyrin-Based Materials−Highlight. *CrystEngComm* **2002**, *4*, 109−116.

(24) Shmilovits, M.; Diskin-Posner, Y.; Vinodu, M.; Goldberg, I. Crystal-engineering of porphyrin sieves based on coordination polymers of Pd- and Pt- tetra(4-carboxyphenyl)porphyrin. *Cryst. Growth Des.* **2003**, *3*, 855−863.

(25) Bhyrappa, P.; Wilson, S. R.; Suslick, K. S. Hydrogen Bonded Porphyrinic Solids: Supramolecular networks of octahydroxy porphyrins. *J. Am. Chem. Soc.* **1997**, *119*, 8492−8502.

(26) Bhyrappa, P.; Suslick, K. S. Surpramolecular networks of octahydroxy porphyrins. *Supramol. Chem.* **1998**, *9*, 169−174.

(27) Kosal, M. E.; Suslick, K. S. Microporous porphyrin and metalloporphyrin materials. *J. Solid State Chem.* **2000**, *152*, 87−98.

(28) Suslick, K. S.; Rakow, N. A.; Kosal, M. E.; Chou, J.-H. The materials chemistry of porphyrins and metalloporphyrins. *J. Porphyrins Phthalocyanines* **2000**, *4*, 407−413.

(29) Kosal, M. E.; Chou, J.-H.; Wilson, S. R.; Suslick, K. S. A functional zeolite analogue assembled from metalloporphyrins. *Nat. Mater.* **2002**, *1*, 118−121.

(30) Kosal, M. E.; Chou, J. H.; Suslick, K. S. A calcium-bridged porphyrin coordination network. *J. Porphyrins Phthalocyanines* **2002**, *6*, 377−381.

(31) Kosal, M. E.; Nakagaki, S.; Wilson, S. R.; Suslick, K. S., unpublished data.

(32) Smithenry, D. W.; Wilson, S. R.; Suslick, K. S. A robust microporous zinc porphyrin framework solid. *Inorg. Chem.* **2003**, *42*, 7719−7721.

(33) Sheldon, R. A. In *Metalloporphyrins In Catalytic Oxidations*; Sheldon, R. A., Ed.; Marcel Dekker: New York, 1994.

(34) Suslick, K. S. Shape Selective oxidation by metalloporphyrins. In *The Porphyrin Handbook*; Kadish, K. M., Smith, K. M., Guilard, R., Eds.; Academic Press: New York, 2000; Vol. 4, Chapter 28, pp 41−63.

(35) Sen, A.; Suslick, K. S. Shape-selective discrimination of small organic molecules. *J. Am. Chem. Soc.* **2000**, *122*, 11565−11566.

(36) Bhyrappa, P.; Young, J. K.; Moore, J. S.; Suslick, K. S. Dendrimer-metalloporphyrins: synthesis and catalysis. *J. Am. Chem. Soc.* **1996**, *118*, 5708−5711.

(37) Bhyrappa, P.; Vaijayanthimala, G.; Suslick, K. S. Shape-selective ligation to dendrimer-metalloporphyrins. *J. Am. Chem. Soc.* **1999**, *121*, 262−263.

(38) Zimmerman, S. C.; Wendland, M. S.; Rakow, N. A.; Zharov, I.; Suslick, K. S. Synthetic hosts by monomolecular imprinting inside dendrimers. *Nature* **2002**, *418*, 399−403.

(39) Zimmerman, S. C.; Zharov, I.; Wendland, M. S.; Rakow, N. A.; Suslick, K. S. Molecular imprinting inside dendrimers. *J. Am. Chem. Soc.* **2003**, *125*, 13504−13518.

(40) Chen, B.; Eddaoudi, M.; Kim, J.; Rosi, N.; Vodak, D.; Wachter, J.; O'Keeffe, M.; Yaghi, O, M. Interwoven metal- organic framework on a periodic minimal extra-large pores. *Science* **2002**, *295*, 469−472.

(41) Reichardt, C. Solvatochromic dyes as solvent polarity indicators. *Chem. Rev.* **1994**, *94*, 2319−2358.

AR040173J